Interfacial interaction and glassy dynamics in stacked thin films of poly(methyl methacrylate)

Tatsuhiko Hayashi, Kenta Segawa, Koichiro Sadakane, Koji Fukao, and Norifumi L. Yamada

Citation: J. Chem. Phys. **146**, 203305 (2017); doi: 10.1063/1.4974835
View online: http://dx.doi.org/10.1063/1.4974835
View Table of Contents: http://aip.scitation.org/toc/jcp/146/20
Published by the American Institute of Physics

Interfacial interaction and glassy dynamics in stacked thin films of poly(methyl methacrylate)

Tatsuhiko Hayashi,[1] Kenta Segawa,[1] Koichiro Sadakane,[1,a)] Koji Fukao,[1,b)] and Norifumi L. Yamada[2]

[1]*Department of Physics, Ritsumeikan University, Noji-Higashi 1-1-1, Kusatsu 525-8577, Japan*

[2]*Neutron Science Division, Institute for Materials Structure Science, High Energy Acceleration Research Organization, 203-1 Shirakata, Tokai, Naka 319-1106, Japan*

(Received 27 October 2016; accepted 4 January 2017; published online 2 February 2017)

Neutron reflectivity and dielectric permittivity of alternately stacked thin films of protonated and deuterated poly(methyl methacrylate) were measured to elucidate a correlation between the time evolution of the interfacial structure and the segmental dynamics in the stacked thin polymer films during isothermal annealing above the glass transition temperature. The roughness at the interface between two thin layers increases with the annealing time, whereas the relaxation rate and strength of the α-process decrease with an increase in the annealing time. A strong correlation between the time evolution of the interfacial structure and the dynamics of the α-process during annealing could be observed using neutron reflectivity and dielectric relaxation measurements. *Published by AIP Publishing.* [http://dx.doi.org/10.1063/1.4974835]

I. INTRODUCTION

Mechanical and thermal stability, especially, the glass transition behavior of thin polymer films are important factors in the application of polymeric materials.[1] Since the discovery of a strong deviation of the glass transition temperature T_g in thin polymer films from that of the bulk,[2] there has been much research on the glass transition and dynamics in thin polymer films using various experimental techniques.[3,4] The results mainly support the existence of a distinct deviation of the glass transition temperature from the bulk values, although there are some exceptions.[5,6] There are several candidates for the physical origin of the deviation of T_g, including confinement effects,[7] surface and interfacial effects,[8] the effects of residual stress and solvents,[9] and the effect of adsorbed layer formation.[10] Recently, the non-equilibrium behavior of T_g deviation from that in the bulk and its relationship with the formation of adsorbed layers have been discussed for some cases.[11] Various experiments have shown that enhanced mobility near a free surface can exceed the bulk mobility by several orders of magnitude and can extend for several nanometers into the bulk polymer, as discussed in the review by Ediger and Forrest.[8]

In our previous papers,[12–16] T_g and the α-process of stacked ultrathin polymer layers with thicknesses of several tens of nanometers were investigated when annealed above T_g, to elucidate the effect of the interface on T_g and on the dynamics of the α-process in thin polymer films. There are many interfaces between the thin polymer layers in stacked thin polymer films, which can be regarded as an ideal system to investigate the interfacial effects on the glass transition dynamics. Thermal measurements using differential scanning calorimetry (DSC) revealed that T_g for as-stacked 13-nm-thick films of polystyrene (PS) is approximately 26 K lower than that of the bulk, and T_g increases with the annealing time during the isothermal annealing process and approaches T_g for the bulk,[13] which is consistent with previous reports by Koh and Simon.[17,18] Furthermore, dielectric relaxation spectroscopy (DRS) measurements on stacked thin films of poly(2-chlorostyrene) (P2CS)[12,13] and poly(methyl methacrylate) (PMMA)[16] show that the dynamics of the α-process changes from thin-film-like dynamics (Arrhenius type temperature dependence of the relaxation time for the α-process, τ_α) to bulk-like dynamics (Vogel-Fulcher-Tammann type temperature dependence of τ_α[19–22]) with an increase in the annealing time. Therefore, the deviation of T_g and τ_α in thin polymer films from those of the bulk system can be considered to be strongly associated with the change in the interfacial interaction or the structure of the interfaces between thin polymer layers. Direct measurement of the structural changes at the interface between thin polymer layers within stacked thin polymer films has thus been highly desired, in addition to DSC and DRS measurements.

The time evolution of the interface between two polymer layers, i.e., the interdiffusion of polymers, has widely been studied using various experimental techniques.[23–32] In particular, neutron reflectivity (NR) is a powerful method for the investigation of buried interfaces in multilayered thin films.[33] A combination of NR with deuterium labeling has enabled the precise measurement of interdiffusion between two polymer layers in various polymeric systems.[29–32]

In the present study, direct observation of the time evolution of the interfacial structure between thin polymer layers within stacked thin polymer films during isothermal annealing was performed using NR measurements. DRS measurements of the α-process on the same stacked thin polymer films during

a)Present address: Faculty of Life and Medical Sciences, Doshisha University, Kyotanabe 610-0321, Japan.
b)Author to whom correspondence should be addressed. Electronic mail: fukao.koji@gmail.com.

the annealing process were also performed. Through combined NR and DRS measurements, we have attempted to elucidate how the change in the interfacial structure between two layers is associated with the change in the dynamics of the α-process or the segmental motion of polymer chains in a stacked thin film geometry. The experimental details are described in Sec. II, and the results obtained for 2- and 5-layered thin films of deuterated PMMA (d-PMMA) and protonated PMMA (h-PMMA) are given in Secs. III A and III B, respectively. DRS results for 5-layered thin films are given in Sec. III C. In Sec. III D, a comparison of the results from NR and DRS is given before the concluding remarks.

II. EXPERIMENTAL

A. Sample

The polymer samples used in this study were atactic h-PMMA and d-PMMA, purchased from Polymer Source, Inc. The respective weight-averaged molecular weight, M_w, and the number-averaged molecular weight, M_n, were 1.826×10^6 and 1.304×10^6 for h-PMMA, and 1.558×10^6 and 8.20×10^5 for d-PMMA. Figure 1 shows the chemical structure of d-PMMA, where five of the eight hydrogen atoms of the monomer unit are replaced by deuterium. The scattering length densities (SLD) of h-PMMA and d-PMMA are 1.14×10^{10} cm^{-2} and 4.70×10^{10} cm^{-2}, respectively. T_g for bulk h-PMMA and d-PMMA used in this study were 398.3 K and 401.5 K, respectively, which were measured by DSC during heating at 10 K/min after cooling down from 493 K to room temperature at 10 K/min. The peak temperature of the dielectric loss due to the α-process T_α at 20 Hz is 391.0 K and 391.9 K for the 22-nm-thick film of h-PMMA and the 27-nm-thick film of d-PMMA, respectively.

Two different types of alternately stacked thin films of d-PMMA and h-PMMA were prepared for NR measurements. The thin films were prepared on glass substrates by spin-coating solutions of 0.5 wt. % d-PMMA or h-PMMA in toluene. The film thickness was evaluated directly by atomic force microscopy (AFM) measurements. A d-PMMA film was floated onto a water surface and transferred to the top of a glass substrate. An h-PMMA film was then floated onto the water surface and transferred to the top of the d-PMMA layer on the glass substrate to form a 2-layered thin film of d-PMMA and h-PMMA (2-layered thin film). In addition, three films of d-PMMA, h-PMMA, and d-PMMA were stacked in this order on the 2-layered thin film, which yielded 5-layered thin films consisting of alternately stacked d-PMMA and h-PMMA layers (5-layered thin film). The present geometry of the 2- and 5-layered thin films of d-PMMA and h-PMMA was used for NR measurements to obtain structural information from each layer separately.[34–36] As-stacked thin films were annealed at 333 K for several hours prior to NR measurements.

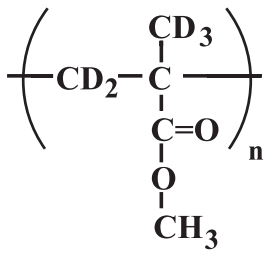

FIG. 1. Chemical structure of d-PMMA used in the present measurements.

For DRS measurements, 5-layered thin films of d-PMMA and h-PMMA with the same geometry as that for the NR measurements were prepared on an aluminum-deposited glass substrate. Aluminum was then vacuum deposited on the 5-layered thin film to serve as an upper electrode.[37,38] The thicknesses of the d-PMMA and h-PMMA layers measured by AFM were 27 and 22 nm, respectively. The samples for DRS measurements were also annealed below 350 K to stabilize them before measurements, as described in Sec. II C.

B. NR measurements

Time-resolved specular NR measurements were performed on a reflectometer, the Soft Interface Analyzer (SOFIA, BL-16, Materials and Life Science Facility, Japan Proton Accelerator Research Complex, Tokai, Japan), with polychromatic wavelengths ranging from 0.25 to 1.76 nm (double frame mode).[39,40] The modulus of the neutron scattering vector in NR is $q = \frac{4\pi}{\lambda} \sin\theta$, where θ is the specular reflection angle and λ is the wavelength of neutrons. θ was set to 0.80° to obtain a q range of 0.1 nm$^{-1} < q < 0.7$ nm^{-1}. Two types of NR samples were mounted on the temperature controllable sample cell. NR measurements were conducted during isothermal annealing at 409 K. The annealing time t_a is defined as the time elapsed from when the temperature of the sample reaches 409 K. Observed reflectivity profiles were analyzed using Motofit[41] within the IGOR software package to evaluate various parameters such as roughness and thickness for characterization of the interface.

As fitting parameters for the 2-layered thin films, we evaluate two thicknesses of the d-PMMA layer (d_d) and the h-PMMA layer (d_h), and two interfacial roughnesses described by an error function between the d-PMMA and h-PMMA layers ($r_{h/d}$), and between the h-PMMA layer and air ($r_{a/h}$), as shown in the inset of Fig. 2. For the 5-layered thin films, fitting parameters were five thicknesses of the top first d-PMMA layer (d_1), the second h-PMMA layer (d_2), the third d-PMMA layer (d_3), the fourth h-PMMA layer (d_4), and the bottom fifth d-PMMA layer (d_5), in addition to five roughnesses, r_i ($i = 1, 2, \ldots, 5$), as shown in the inset of Fig. 5. The r_1 value corresponds to the roughness between air and the top d-PMMA layer, and the r_i values ($i = 2, \ldots, 5$) correspond to the roughness between the ith and $i + 1$th layers. Here, the sixth layer is defined as the glass substrate. For both samples, the roughness between the bottom layer and the substrate was taken into account and was fixed to be a constant value (1.2 nm).

C. DRS measurements

DRS measurements were performed using an LCR meter (Agilent Technologies 4292A). The measured frequency range was from 20 Hz to 1 MHz and the temperature range was from 273 K to 409 K. The complex dielectric permittivity $\varepsilon^*(\omega)$ was obtained from the DRS measurements, where $\omega = 2\pi f$ and f is the frequency of the applied electric field. Prior to DRS measurements, the temperature of the as-prepared 5-layered thin films of d-PMMA and h-PMMA was

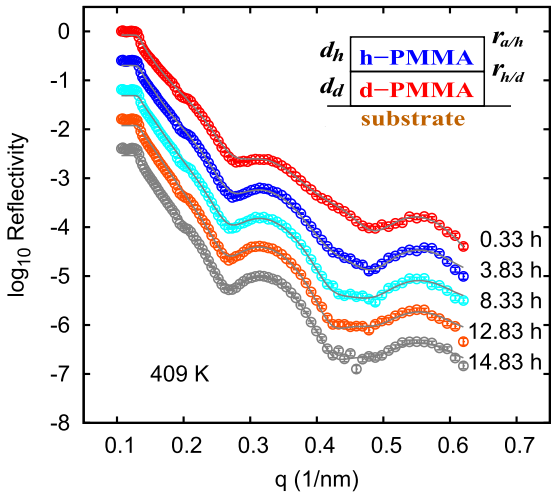

FIG. 2. Dependence of NR on the modulus of the scattering vector q, for 2-layered thin films of d-PMMA and h-PMMA during isothermal annealing at 409 K. The different colored symbols represent the reflectivity profiles at various annealing times from 0.33 h to 14.83 h. Each curve, except for that with $t_a = 0.33$ h, is shifted along the vertical axis by a certain amount to avoid data overlap.

changed between 273 K and 350 K at a rate of 1 K/min to stabilize the samples. The following temperature cycle was then repeated approximately 40 times. One cycle consists of two steps: (1) cooling and heating processes between 409 K and 273 K at 1 K/min are performed twice and (2) the temperature is held at 409 K for 1 h after the ramping process. As discussed in Ref. 13, the sum of the time for which the sample is held at 409 K can be regarded as the annealing time t_a, because the effect of annealing during the ramping processes can be neglected.

III. RESULTS AND DISCUSSION

A. NR of 2-layered thin films

Figure 2 shows the dependence of NR on the modulus of the scattering vector q for 2-layered thin films at various annealing times from 0.33 h to 14.83 h during isothermal annealing at 409 K. Kiessig fringes are observed in Fig. 2. The shape for the q range of 0.3 $nm^{-1} < q < 0.5$ nm^{-1} has been changed with an increase in the annealing time. The solid curves in Fig. 2 show that the observed q dependence of the neutron reflectivity can be well reproduced using a model function for the 2-layered thin films that include two thicknesses and three roughnesses, one at the substrate surface, one at the air surface, and one between the film layers. Here, the roughness at the substrate surface is fixed to be 1.2 nm, which was obtained by data fitting over a wider q-range. As a result, four quantities $r_{h/d}$, $r_{a/h}$, d_d, and d_h were successfully evaluated as a function of the annealing time, t_a.

Figure 3 shows the roughness in the 2-layered thin films as a function of the annealing time at 409 K for the interface between air and the h-PMMA layer $r_{a/h}$, and that between the d-PMMA and h-PMMA layers $r_{h/d}$. In Fig. 3, $r_{a/h}$ remains almost unchanged during the annealing, while the roughness $r_{h/d}$ increases with the annealing time. This result suggests that the interdiffusion of polymer chains occurs at the interface

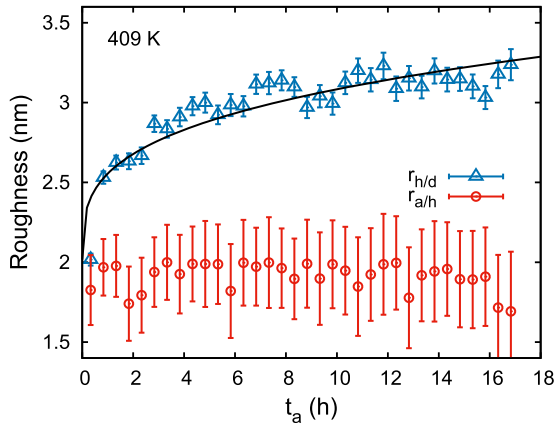

FIG. 3. Roughness as a function of the annealing time observed at the two different interfaces: between air and the h-PMMA layer (red open circle) and between the d-PMMA and h-PMMA layers (blue open triangle). The curve is given by $r_{h/d}(t_a) = r^0_{h/d} + \Delta r_{h/d} t_a^{\alpha}$, where $r^0_{h/d} = 2.0 \pm 0.1$, $\Delta r_{h/d} = 0.54 \pm 0.09$, and $\alpha = 0.30 \pm 0.02$.

between the d-PMMA and h-PMMA layers and the diffusion length at the interface could be larger than the surface roughness at the surface of the top h-PMMA layer.[31]

Figure 4 shows thicknesses of the d-PMMA layer d_d, and the h-PMMA layer d_h, in the 2-layered thin films as a function of the isothermal annealing time. The average thickness between the d-PMMA and h-PMMA layers is also shown as a function of the annealing time in Fig. 4. The thickness d_d increases with the annealing time, while the thickness d_h decreases with an increase in the annealing time. Furthermore, the average thickness between the layer thicknesses of the d-PMMA and h-PMMA layers, i.e., the total thickness of the 2-layered thin films, remains almost unchanged. These experimental results suggest that, in addition to the increase in the width of the interfacial region between the d-PMMA and h-PMMA layers, the averaged position of the interface is shifted from the d-PMMA side to the h-PMMA side during the isothermal annealing process. At the same time, the total thickness of the 2-layered thin films remains almost constant, which

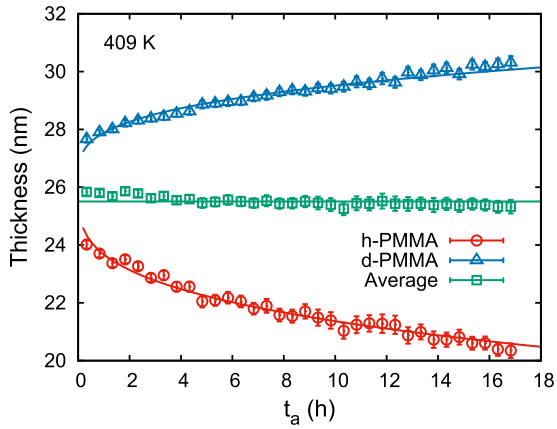

FIG. 4. Thicknesses of the d-PMMA (blue open triangle) and h-PMMA (red open circle) layers in 2-layered thin films of d-PMMA and h-PMMA as a function of the annealing time at 409 K. The average thickness between the d-PMMA and h-PMMA layers is also shown (green open box). The curves are given by $d_d(t_a) = d^0_d + \Delta d_d t_a^{\alpha}$ and $d_h(t_a) = d^0_h - \Delta d_h t_a^{\alpha}$, where $d^0_d = 26.2 \pm 0.3$, $\Delta d_d = 1.7 \pm 0.2$, $d^0_h = 26.0 \pm 0.4$, $\Delta d_h = 2.3 \pm 0.3$, and $\alpha = 0.30 \pm 0.02$.

implies that the time evolution of the layered thin film structure occurs only within the layered thin film itself. The layered thin films prepared by stacking thin films floated on water surface could possibly have included water molecules at the interface between the two thin layers. However, the constant total thickness of the 2-layered thin films during annealing indicates that no water molecules were included, because the total thickness would change with the annealing time if water molecules were included within the 2-layered thin films. In addition to these reasons, there are two other reasons for no water molecules as follows: (1) PMMA is hydrohobic, and hence water should be segregated during stacking procedures, and (2) there is no large dielectric loss signal related to polar water molecules.

It should be noted here that the constancy of the total thickness of 5-layered thin films is better than that of 2-layered thin films, as shown in Fig. 7. If there were water molecules at the interface between thin polymer layers, the constancy of the total thickness of 5-layered thin films should be worse than that of 2-layered thin films. However, this is not the case for the present experimental results.

A possible explanation for the observed time evolution of the d_d and d_h layer thicknesses is given as follows. If the 2-layered thin films are formed by two polymeric systems with different dynamical properties, such as different molecular weights and/or different T_g, then interdiffusion at the interface exhibits an asymmetric dynamical character.[30,32] An interdiffusion model proposed by Jabbari and Peppas[42] describes this asymmetric diffusion. In this model, one phase consists of a polymer with low mobility (slow component) and the other phase consists of a polymer with high mobility (fast component). The time derivative of density of one component (slow component) can be described by the sum of two terms, where one term corresponds to the interdiffusion at the interface between the two polymers and the other term corresponds to the swelling of the slower component by the faster component. In this case, the interface defined as the depth at $\phi = 0.5$ is shifted to the faster component side with an increase in the annealing time. Here, ϕ is a fraction of the slow component. In the present case, T_g of bulk d-PMMA is 3.2 K higher than that of h-PMMA. The d-PMMA and h-PMMA layers can be regarded as the slow and fast components, respectively. If this model is valid, then the thickness of the d-PMMA layer should increase with the annealing time due to swelling of the slower component (the d-PMMA layer) by the faster component (the h-PMMA layer), which is consistent with the observed time evolution of the d-PMMA layer thickness.

B. NR of 5-layered thin films

In Sec. III A, the time evolution of the interface of the 2-layered thin films was discussed and the characteristic change in the roughness and thickness of the d-PMMA and h-PMMA layers was clarified. Here, the NR results for the 5-layered thin films are also shown, and the interfacial structures are discussed to extract common properties between the 2- and 5-layered thin films. Figure 5 shows the NR profiles for the 5-layered thin films with respect to q at various annealing times during annealing at 409 K. The dependence of the NR profile on q in the range of 0.25 $nm^{-1} < q < 0.35$ nm^{-1} clearly changes with an increase in the annealing time. The solid

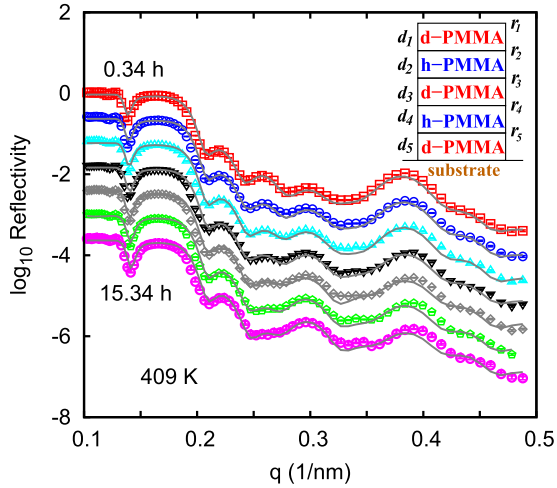

FIG. 5. NR profiles with respect to the modulus of the scattering vector q for 5-layered thin films of d-PMMA and h-PMMA during isothermal annealing at 409 K. The different colored symbols represent the reflectivity profiles at various annealing times of 0.34, 1.34, 2.34, 3.84, 5.34, 8.34, and 15.34 h. The curves were evaluated using data fitting with a model function. Each curve is shifted along the vertical axis by a certain amount to avoid data overlap.

curves show that the observed q dependence of the NR profile can well be reproduced using a model function that includes five roughnesses r_i and five thicknesses, d_i ($i = 1, \ldots, 5$) as fitting parameters, in addition to one roughness at the substrate surface.

Figure 6 shows the dependence of the roughness on the annealing time at various positions within the 5-layered thin films during annealing. Four distinct roughnesses at the interfaces between the d-PMMA and h-PMMA layers, r_2, r_3, r_4, and r_5, increase with the annealing time. Before the measurements, we expected that there is positional dependence of roughnesses at the interfaces between thin polymer layers. However, there is not enough resolution to detect the positional dependence, because of some data scatters due to the large number of fitting parameters. Nevertheless, the averaged roughness exhibits a distinct increase with the annealing time, which confirms that the roughness observed for the 5-layered

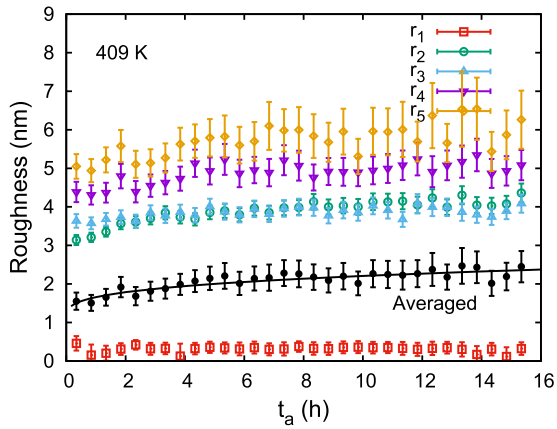

FIG. 6. Dependence of the roughness on the annealing time observed at various positions within the 5-layered thin films of d-PMMA and h-PMMA during isothermal annealing at 409 K. The averaged roughness (r_{ave}, •) is shifted by −2.5 nm along the vertical axis to avoid data overlap. The curve for r_{ave} is given by $r_{ave}(t_a) = r^0_{ave} + \Delta r_{ave} t_a^{\alpha}$, where $r^0_{ave} = 3.59 \pm 0.08$, $\Delta r_{ave} = 0.56 \pm 0.05$, and $\alpha = 0.30$.

thin films is consistent with that observed for the 2-layered thin films.

Figure 7 shows the dependence of the thicknesses on the annealing time for two h-PMMA layers and three d-PMMA layers in the 5-layered thin films. The thicknesses of the h-PMMA layers, d_2 and d_4, decrease with an increase in the annealing time, while the thicknesses of the d-PMMA layers, d_1 and d_5, increased slightly with the annealing time, although there are large error bars that could obscure the dependence on the annealing time. In contrast to d_1 and d_5, the thickness of the third d-PMMA layer, d_3, increases with the annealing time in a more distinct manner. If the increase in the thickness of the d-PMMA layer is due to the swelling of the d-PMMA layer by the entering of the h-PMMA component into the d-PMMA layer, then the observed difference between d_1 (or d_5) and d_3 is reasonable, because the third d-PMMA layer is covered with h-PMMA layers on both sides, and the first and fifth d-PMMA layers are covered with a h-PMMA layer on only one side. The black curve in Fig. 7 shows that the average thickness over the five layers remains almost independent of the annealing time, in a similar manner to that observed for the 2-layered thin films. Here, it should be noted that the amount of change in d_1 (or d_5) is smaller than that expected from the NR results for 2-layered thin films, and that the surface roughness of 5-layered thin films is smaller than that of 2-layered thin films. This might come from an incomplete fine tuning of fitting parameters, because the number of fitting parameters for 5-layered thin films is larger than that for 2-layered thin films.

Based on these results, we can expect that the observed dependence of thickness and roughness on the annealing time for the d-PMMA and h-PMMA layers in the 5-layered thin films would be the same as that for the 2-layered thin films. Thus, the time evolution of the interfacial structure observed for the 2-layered thin films should also occur for the 5-layered thin films.

C. DRS of 5-layered thin films

The NR measurements reported in Secs. III A and III B show that there is characteristic time evolution of the interfacial structure for both the 2-layered and 5-layered thin films during isothermal annealing at 409 K. The dynamical change that could occur together with the interfacial change during annealing was also investigated using DRS. *In situ* DRS measurements were performed on the 5-layered thin films of d-PMMA and h-PMMA during the annealing process.

Figure 8 shows the temperature dependence of the imaginary part of the dielectric permittivity ε'' for the 5-layered thin films measured at 20 Hz with various annealing times from 0 to 39 h during annealing at 409 K. Two contributions are evident in the spectra; the α-process (segmental motion) and β-process (local motion) were observed, similar to the stacked thin films of h-PMMA layers (without d-PMMA layers) reported previously.[16,43]

To discuss the time evolution of segmental motion during the annealing process, the dielectric relaxation strength $\Delta\varepsilon_\alpha$ and the peak temperature of the α-process T_α at 20 Hz were evaluated from the dielectric loss spectra in the temperature domain given in Fig. 8. Data fitting using a model function consisting of the α- and β-processes with various parameters such as the temperature, width, and height of the loss peaks for each component. The detailed procedure is given in Ref. 16. Figure 9 shows that the peak temperature of the α-process T_α increases with the annealing time, while the dielectric relaxation strength of the α-process decreases with an increase in the annealing time. The dependence of T_α and $\Delta\varepsilon_\alpha$ on the annealing time suggests that the dynamics of the α-process for as-stacked thin films of d-PMMA and h-PMMA changes from thin-film-like dynamics to bulk-like dynamics during the annealing process above T_g. The observed dependence of T_α and $\Delta\varepsilon_\alpha$ on the annealing time for the 5-layered thin films of d-PMMA and h-PMMA is similar to that observed for stacked thin films of h-PMMA layers.

D. Comparison of DRS and NR results

In Secs. III A, III B, and III C, we have observed the annealing time dependence of the roughness, $r_{h/d}$, and thickness, d_d, d_h, and d_3, for the 2-layered and 5-layered thin films by NR measurements and that of the dielectric relaxation strength $\Delta\varepsilon_\alpha$ and the α-peak temperature T_α by DRS measurements during annealing at 409 K. Each physical quantity exhibits a characteristic dependence on the annealing time, t_a. Here, we describe the annealing time dependence of a quantity

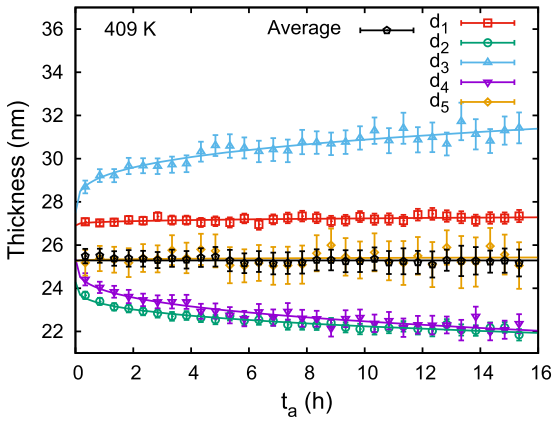

FIG. 7. Dependence of the layer thickness on the annealing time observed at various positions within the 5-layered thin films of d-PMMA and h-PMMA during isothermal annealing at 409 K. The averaged thickness is also plotted (•). The curve for d_3 is given by $d_3(t_a) = d_3^0 + \Delta d_3 t_a^\alpha$, where $d_3^0 = 27.5 \pm 0.2$, $\Delta d_3 = 1.7 \pm 0.1$, and $\alpha = 0.30 \pm 0.02$.

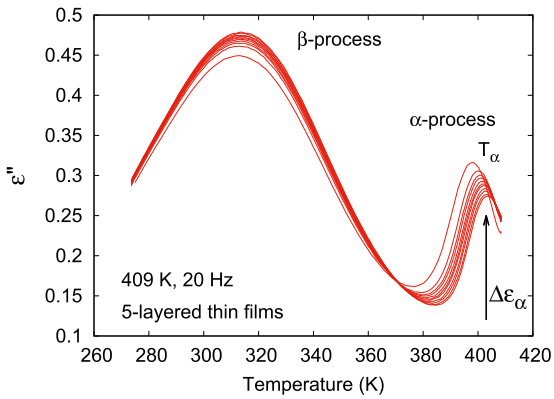

FIG. 8. Dielectric loss spectra (20 Hz) in the temperature domain for the 5-layered thin films of d-PMMA and h-PMMA annealed at 409 K for various annealing times, 0, 1, 2, 3, 5, 7, 9, 14, 19, 29, and 39 h.

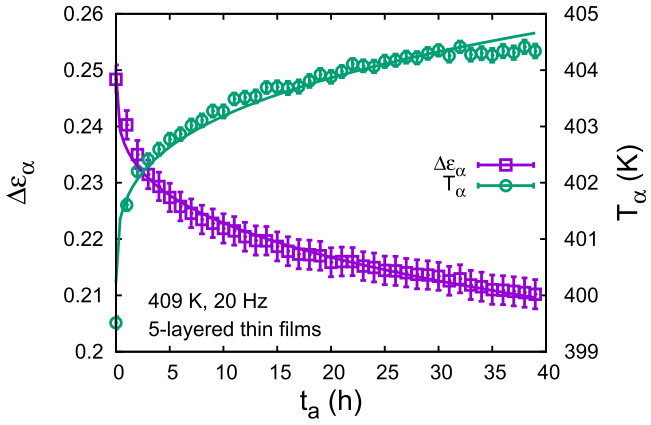

FIG. 9. Annealing time dependence of the dielectric strength of the α-process $\Delta\varepsilon_\alpha$ at 20 Hz, and the temperature T_α at which the dielectric loss shows a peak due to the α-process at 20 Hz for the 5-layered thin films of d-PMMA and h-PMMA. The curves are evaluated by $\Delta\varepsilon_\alpha(t_a) = \Delta\varepsilon_\alpha^0 - \Delta\tilde{\varepsilon}_\alpha t_a^\alpha$ and $T_\alpha(t_a) = T_\alpha^0 + \Delta T_\alpha t_a^\alpha$, where $\Delta\varepsilon_\alpha^0 = 0.25$, $\Delta\tilde{\varepsilon}_\alpha = 0.013$, $T_\alpha^0 = 400.2 \pm 0.9$, $\Delta T_\alpha = 1.5 \pm 0.4$, and $\alpha = 0.30 \pm 0.02$.

X ($\equiv\Delta\varepsilon_\alpha$, T_α, $r_{h/d}$, d_d, d_h, and d_3) as follows:

$$X(t_a) = X_0 + \Delta X \zeta(t_a), \tag{1}$$

where X_0 is the initial value, ΔX is the strength of the relaxation and/or diffusion, and $\zeta(t_a)$ is a reduced function describing the time evolution of the quantity X. If Eq. (1) with a common function $\zeta(t_a)$ can reproduce the observed dependence of the X quantities on the annealing time, including those observed using DRS and NR, we could conclude that there is a universal physical process behind the DRS and NR results.

Here, it is assumed that the function $\zeta(t_a)$ is given by a power law t_a^α with a common exponent of α over six different X quantities. In order to check the validity of this assumption, we made data fitting for the dependences of all six X quantities on the annealing time *simultaneously* using six sets of Eq. (1) with individual parameters X_0 and ΔX, and with *a common parameter* α. As a result, the common value of α could be obtained as follows:

$$\alpha = 0.30 \pm 0.02. \tag{2}$$

The reproducibility of the observed dependence of the six quantities on the annealing time can be checked by comparing the observed data with calculated curves in Figs. 3, 4, 7, and 9. In the present annealing time range, the dependence of the six quantities on the annealing time can be well reproduced by a common time evolution described by $\zeta(t_a) = t_a^\alpha$ with $\alpha = 0.30$.

For each quantity X, we can convert the observed values of X into the values of $\zeta(t_a)$ using fitting parameters X_0 and ΔX. Figure 10(a) shows the dependence of the reduced function ζ on the annealing time for six different quantities, $\Delta\varepsilon_\alpha$, T_α, $r_{h/d}$, d_d, d_h, and d_3 for the 2-layered and 5-layered thin films during the annealing at 409 K. Although there are some scatters in data points, especially for d_3 in the 5-layered thin films, the six different quantities can be well reduced into a single master curve; therefore, there is a clear similarity in the time evolution of the six different quantities observed from both NR and DRS measurements. Therefore, it can be concluded that *the time evolution of the segmental motion observed by DRS is strongly associated with that of the interfacial structure observed with NR during the isothermal annealing process*. This result suggests that the thin-film-like glassy dynamics observed for the stacked thin films of polymeric systems such as PMMA, PS, and P2CS are due to the existence of interfacial regions between the two thin layers, and their disappearance can change the thin-film-like glassy dynamics into bulk-like glassy dynamics, which has been observed with several measurements.[12,13,16,17]

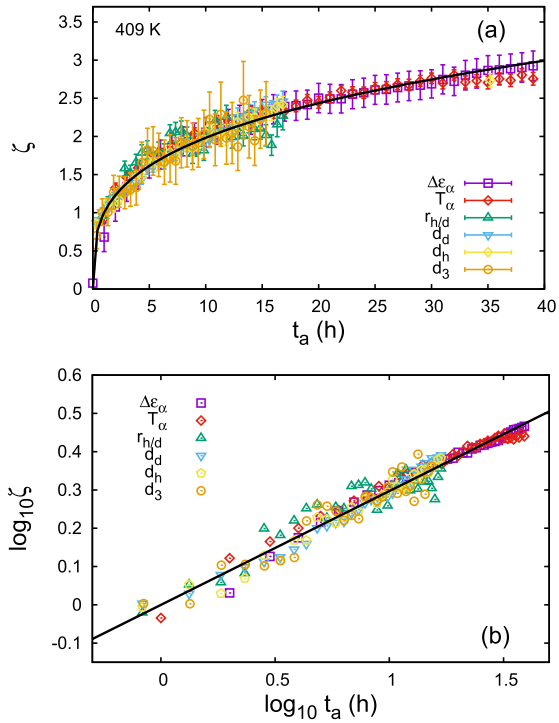

FIG. 10. Annealing time dependence of the scaled function ζ for the dielectric strength $\Delta\varepsilon_\alpha$, the α-peak temperature T_α, the roughness at the interface between d-PMMA and h-PMAA in the 2-layered thin films $r_{h/d}$, the thicknesses of the d-PMMA and h-PMMA layers in the 2-layered thin films d_d and d_h, the thickness of the third layer in the 5-layered thin films d_3, observed during isothermal annealing at 409 K; (a) linear and (b) double logarithmic plots. The values of $\Delta\varepsilon_\alpha$ and T_α were evaluated using DRS, and those of $r_{h/d}$, d_d, d_h, and d_3 were determined from NR measurements. The solid curves in (a) and (b) are given by $\zeta(t_a) = t_a^\alpha$, where $\alpha = 0.30 \pm 0.02$.

Figure 10(b) shows the annealing time dependence of $\zeta(t_a)$ on a double logarithmic scale to discuss the underlying time evolution of the X quantities. Here, the physical meaning of the power law with the exponent $\alpha = 0.30$ is discussed. In the present case, the reptation time τ_d can be evaluated using the equation $\tau_d = 2R_g^2/\pi^2 D_{rept}$ according to the standard theory proposed by Doi and Edwards,[44] where R_g is the radius of gyration of the polymer chain in question and D_{rept} is the diffusion constant due to the reptation dynamics. For d-PMMA used in this study, R_g and D_{rept} can be evaluated as follows: $R_g = 28.1$ nm for $M_n = 8.20 \times 10^5$ using the relation $R_g = 0.031 \times M_n^{1/2}$,[45] and $D_{rept} = 2.5 \times 10^{-19}$ cm^2/s at 409 K, from the observed tracer diffusion coefficient at 418 K for PMMA with $M_n = 4.91 \times 10^5$ [46] after correction using the shift factor $\log a_T = c_1^0(T - T_0)/(c_2^0 + T - T_0)$ with $c_1^0 = 10.42$, $c_2^0 = 58.5$ K, and $T_0 = 403$ K.[31,47] As a result, the reptation time for the present case is evaluated as $\tau_d = 1775$ h. τ_d is located far above the observed range of the annealing time; therefore,

the translational motion of the polymer in this case could be controlled by Rouse motion. The reptation and Rouse dynamics predict that the time dependence of the root mean square displacement should follow a power law $t^{1/4}$ for the time range shorter than τ_d (and larger than the Rouse time). Although it is difficult to judge the validity of the present discussion because of the scatters in the data point in Fig. 10(b), the observed value of $\alpha = 0.30$ can be comparable to the predicted value of $\alpha = 1/4$ due to the Rouse dynamics. Hence, the time evolution observed at the interface during the annealing may be governed by the Rouse dynamics. Similar behaviors have been observed at the interface in previous studies.[31,32]

As discussed in Sec. III A, asymmetric interdiffusion was observed in the present case. Therefore, if there is an asymmetry effect in the diffusion motion near the interface, then the annealing time dependence of the mean square displacement can be modified.[30,32] This could be a possible reason for the deviation of the exponent α observed in the present measurements from the theoretically predicted value.

In Fig. 10(b), we notice that there seems to be a slight deviation from the power-law relation. For $t_a > 17$ h, there are the observed data only from DRS measurements. The glass transition of as-stacked thin polymer films changes into that of the bulk system with annealing,[13,16] and hence, the T_g and T_α should *relax* or saturate to the bulk value. On the other hand, if the reptation model is valid in this case, the mean squared displacement should increase as a linear function of t_a in the longer time region, which leads to an increase in slope in Fig. 10(b). Below $t_a < 17$ h, we could observe a nice agreement between the time evolutions of the DRS and NR results, while above $t_a > 17$ h there might be a possibility of separation into two different time evolutions.

IV. CONCLUDING REMARKS

The time evolution of the interfacial structure and the dynamics of stacked PMMA thin films were investigated using NR and DRS measurements. The results obtained are summarized as follows:

1. The dynamics of the α-process for alternately stacked thin films of d-PMMA and h-PMMA layers has thin-film-like behavior. Annealing above T_g causes the α-process to become slower and approach the bulk α-process.
2. Interfacial structures, such as the roughness and the position of the averaged interface in the stacked thin films, change with an increase in the annealing time.
3. The characteristic time scales and time evolution obtained from NR and DRS measurements were the same; therefore, the interdiffusion of polymer chains occurs at the interface with almost the same characteristic time as the change in the α-dynamics.

In our measurements, the interdiffusion of polymer chains proceeds with increasing annealing time, and we expect that on a final stage of the annealing, a large film with homogeneous structure of d-PMMA and h-PMMA could be obtained. However, during the present annealing process or time range, 2-layered thin films and 5-layered thin films are still highly heterogeneous, while the interfacial structure between polymer thin layers becomes much broader than before the annealing above T_g, and the deviation of T_α and T_g from the bulk values almost disappears. Therefore, the present results suggest that the interface roughening mainly causes the disappearance of T_g depression.

The annealing time dependence of the d-PMMA and h-PMMA layer thicknesses was different for each layer, and the position of the interface was shifted from the d-PMMA side to the h-PMMA side in the present study. Preliminary NR measurement indicated that the position of the interface is shifted from the h-PMMA side to the d-PMMA side during annealing, when T_g for the d-PMMA layer is controlled to be lower than T_g for the h-PMMA layer by blending lower molecular weight d-PMMA into the original d-PMMA. At the present stage, the most probable reason for the shift of the interface is considered to be the asymmetric dynamical properties of d- and h-PMMA layers, as discussed in Sec. III A. In the case of asymmetric interdiffusion at the interface, the error function may not be sufficient to describe the interfacial structure between two polymer layers, but may only be an approximate functional form. For further detailed discussion, the possible deviation from the simple error function should be taken into account for detailed analysis of the NR profiles.

As described in Sec. I, the formation of a non-equilibrium adsorbed layer might play a crucial role for the deviation of T_g from the bulk. Hence, the growth and development of an irreversible adsorbed nanolayer at the polymer-substrate interface due to the annealing above T_g could influence the observed dependence of the structure and dielectric properties of 2-layered thin films, especially. Such an effect due to the formation of a non-equilibrium adsorbed layer should also be discussed to obtain the better understanding of the confinement effects of glass transition and the α-process for polymeric systems.

ACKNOWLEDGMENTS

This work was partly supported by Grants-in-Aid for Scientific Research (B) (Nos. 25287108 and 16H04036) and Exploratory Research (No. 16K13868) from the Japan Society for the Promotion of Science. NR measurements were performed on the BL-16 beamline at the Materials and Life Science Facility, J-PARC, Japan, under Program Nos. 2014B0073 and 2016A0025.

[1] K. L. Ngai, in *Physical Properties of Polymers*, edited by J. Mark (Cambridge University Press, 2004), pp. 72–152.
[2] J. L. Keddie, R. A. L. Jones, and R. A. Cory, Europhys. Lett. **27**, 59 (1994).
[3] J. A. Forrest and R. A. Jones, in *Polymer Surfaces, Interfaces and Thin Films*, Advances in Polymer Science, edited by A. Karim and S. Kumar (World Scientific Publishing, 2000), pp. 251–294.
[4] M. Alcoutlabi and G. B. McKenna, J. Phys.: Condens. Matter **17**, R461 (2005).
[5] M. Y. Efremov, A. V. Kiyanova, J. Last, S. S. Soofi, C. Thode, and P. F. Nealey, Phys. Rev. E **86**, 021501 (2012).
[6] M. Tress, M. Erber, E. U. Mapesa, H. Huth, J. Müller, A. Serghei, C. Schick, K.-J. Eichhorn, B. Voit, and F. Kremer, Macromolecules **43**, 9937 (2010).
[7] B. Jérôme, J. Phys.: Condens. Matter **11**, A189 (1999).
[8] M. D. Ediger and J. A. Forrest, Macromolecules **47**, 471 (2014).
[9] G. Reiter, M. Hamieh, P. Damman, S. Sclavons, S. Gabriele, T. Vilmin, and E. Raphael, Nat. Mater. **4**, 754 (2005).
[10] S. Napolitano, S. Capponi, and B. Vanroy, Eur. Phys. J. E **36**, 61 (2013).

[11]S. Napolitano, *Non-equilibrium Phenomena in Confined Soft Matter*, Soft and Biological Matter (Springer International Publishing, Heidelberg, 2015), ISBN: 978-3-319-21948-6.
[12]K. Fukao, Y. Oda, K. Nakamura, and D. Tahara, Eur. Phys. J.: Spec. Top. **189**, 165 (2010).
[13]K. Fukao, T. Terasawa, Y. Oda, K. Nakamura, and D. Tahara, Phys. Rev. E **84**, 041808 (2011).
[14]K. Fukao, T. Terasawa, K. Nakamura, and D. Tahara, in *Glass Transition, Dynamics and Heterogeneity of Polymer Thin Films*, Advances in Polymer Science Vol. 252, edited by T. Kanaya (Springer Berlin Heidelberg, 2013), pp. 65–106.
[15]K. Fukao, H. Takaki, and T. Hayashi, in *Dynamics in Geometrical Confinement*, Advances in Dielectrics, edited by F. Kremer (Springer International Publishing, 2014), pp. 179–212.
[16]T. Hayashi and K. Fukao, Phys. Rev. E **89**, 022602 (2014).
[17]Y. P. Koh, G. B. McKenna, and S. L. Simon, J. Polym. Sci., Part B: Polym. Phys. **44**, 3518 (2006).
[18]Y. P. Koh and S. L. Simon, J. Polym. Sci., Part B: Polym. Phys. **46**, 2741 (2008).
[19]H. Vogel, Phys. Z. **22**, 645 (1921).
[20]G. Tammann and W. Hesse, Z. Anorg. Allg. Chem. **156**, 245 (1926).
[21]G. S. Fulcher, J. Am. Ceram. Soc. **8**, 339 (1925).
[22]G. S. Fulcher, J. Am. Ceram. Soc. **8**, 789 (1925).
[23]P. F. Green, C. J. Palmstrom, J. W. Mayer, and E. J. Kramer, Macromolecules **18**, 501 (1985).
[24]E. A. Jordan, R. C. Ball, A. M. Donald, L. J. Fetters, R. A. L. Jones, and J. Klein, Macromolecules **21**, 235 (1988).
[25]S. F. Tead and E. J. Kramer, Macromolecules **21**, 1513 (1988).
[26]J. Von Seggern, S. Klotz, and H. J. Cantow, Macromolecules **22**, 3328 (1989).
[27]S. J. Whitlow and R. P. Wool, Macromolecules **22**, 2648 (1989).
[28]S. J. Whitlow and R. P. Wool, Macromolecules **24**, 5926 (1991).
[29]B. B. Sauer and D. J. Walsh, Macromolecules **24**, 5948 (1991).
[30]A. Karim, G. P. Felcher, and T. P. Russell, Macromolecules **27**, 6973 (1994).
[31]K. Kunz and M. Stamm, Macromolecules **29**, 2548 (1996).
[32]D. Kawaguchi, A. Nelson, Y. Masubuchi, J. P. Majewski, N. Torikai, N. L. Yamada, A. R. Siti Sarah, A. Takano, and Y. Matsushita, Macromolecules **44**, 9424 (2011).
[33]N. Torikai, N. L. Yamada, A. Noro, M. Harada, D. Kawaguchi, A. Takano, and Y. Matsushita, Polym. J. **39**, 1238 (2007).
[34]R. Inoue, K. Kawashima, K. Matsui, T. Kanaya, K. Nishida, G. Matsuba, and M. Hino, Phys. Rev. E **83**, 021801 (2011).
[35]R. Inoue, K. Kawashima, K. Matsui, M. Nakamura, K. Nishida, T. Kanaya, and N. L. Yamada, Phys. Rev. E **84**, 031802 (2011).
[36]R. Inoue, M. Nakamura, K. Matsui, T. Kanaya, K. Nishida, and M. Hino, Phys. Rev. E **88**, 032601 (2013).
[37]K. Fukao and Y. Miyamoto, Europhys. Lett. **46**, 649 (1999).
[38]K. Fukao and Y. Miyamoto, Phys. Rev. E **61**, 1743 (2000).
[39]N. L. Yamada, N. Torikai, K. Mitamura, H. Sagehashi, S. Sato, H. Seto, T. Sugita, S. Goko, M. Furusaka, T. Oda *et al.*, Eur. Phys. J. Plus **126**, 108 (2011).
[40]K. Mitamura, N. L. Yamada, H. Sagehashi, N. Torikai, H. Arita, M. Terada, M. Kobayashi, S. Sato, H. Seto, S. Goko *et al.*, Polym. J. **45**, 100 (2013).
[41]A. Nelson, J. Appl. Crystallogr. **39**, 273 (2006).
[42]E. Jabbari and N. A. Peppas, Polymer **36**, 575 (1995).
[43]K. Fukao, S. Uno, Y. Miyamoto, A. Hoshino, and H. Miyaji, Phys. Rev. E **64**, 051807 (2001).
[44]M. Doi and S. F. Edwards, in *The Theory of Polymer Dynamics*, International Series of Monographs on Physics, Vol. 73, 1st ed. (Clarendon Press, Oxford, 1988), ISBN: 0-19-852033-6.
[45]R. G. Kirste, W. A. Kruse, and K. Ibel, Polymer **16**, 120 (1975).
[46]Y. Liu, G. Reiter, K. Kunz, and M. Stamm, Macromolecules **26**, 2134 (1993).
[47]M. L. Williams, R. F. Landel, and J. D. Ferry, J. Am. Chem. Soc. **77**, 3701 (1955).